Electronic structure of graphitic boron at a $TaB_2(0001)$ surface

H. Kawanowa
National Institute for Research in Inorganic Materials 1-1, Namiki, Tsukuba, Ibaraki 305-0044, Japan
and Department of Materials Science and Technology, Science University of Tokyo, Noda, Chiba 278-8510, Japan

R. Souda
National Institute for Research in Inorganic Materials 1-1, Namiki, Tsukuba, Ibaraki 305-0044, Japan

K. Yamamoto
Kanagawa Institute of Technology, 1030 Shimo-Ogino, Atsugi, Kanagawa 243-0292, Japan

S. Otani
National Institute for Research in Inorganic Materials 1-1, Namiki, Tsukuba, Ibaraki 305-0044, Japan

Y. Gotoh
Department of Materials Science and Technology, Science University of Tokyo, Noda, Chiba 278-8510, Japan
(Received 20 November 1998)

The electronic structure of the $TaB_2(0001)$ surface, which is terminated by graphitic boron layer has been investigated by angle-resolved ultraviolet photoelectron spectroscopy and first-principles self-consistent-charge discrete variational-$X\alpha$ calculations. The occurrence of the charge transfer from Ta to B, leading to large work function (5.9 eV) of the $TaB_2(0001)$ surface is confirmed from Mulliken population analysis. It is concluded that the graphitic boron layer at the $TaB_2(0001)$ surface forms π bond, which is largely modified due to hybridization with the Ta $5d$ orbitals. [S0163-1829(99)03328-7]

I. INTRODUCTION

Boron-rich compounds are attractive materials due to its hardness next to diamond, high-melting point and chemical stability. In metal borides MB_2–MB_{66} (M: metal), two or three-dimensional frameworks of boron atoms are contained,[1] forming graphitic layer, octahedral B_6 and icosahedral or cubo-octahedral B_{12} clusters. On the other hand, the boron itself does not form layered structures but consists of B_{12} clusters. The electronic properties of these boron clusters are characterized by the three-center electron-deficient bond.[2] As for the bulk transition-metal diborides (TMB_2), the boron atoms form the graphitic network between the metal layers. So far, nature of the bonding of boron atoms in bulk TMB_2 has been discussed via the band calculations,[3–6] the de Haas-van Alphen effect[7–9] and the x-ray photoemission spectroscopy,[10] etc. The TMB_2 has three types of bonds, boron-boron, metal-metal and boron-metal bonds and many studies have been done concerning that dominant bonding is[11–13] and especially concerning charge transfer between the graphitic boron layer and the metal layer. The most interesting point in this respect is whether the graphitic boron network possesses the isoelectronicity to graphite or not; that is, the negatively charged boron ions can form networks isoelectronic to graphite. On the other hand, very little work has been carried out concerning surface properties of TMB_2, such as atomic structure, electronic structure, chemical reactivity etc. Recently, We investigated the $TaB_2(0001)$ surface by using impact collision ion spectroscopy (ICISS),[14] and found that the graphitic boron layer terminates the $TaB_2(0001)$ surface, where each boron atom locates on every threefold hollow site of the hexagonal closed-packed tantalum layer. The spacing between the boron layer and the tantalum layer is found to be 0.175 ± 0.002 nm, which indicates positive relaxation relative to the bulk TaB_2 crystal by 8.47%. In the present work, we report on the electronic structure of the clean $TaB_2(0001)$ surface by using angle-resolved ultraviolet photoelectron spectroscopy (ARUPS) and self-consistent-charge discrete variational-$X\alpha$ calculations (SCC-DV-$X\alpha$).

II. EXPERIMENT

The experiments were carried out in an ultrahigh vacuum chamber (base pressure $< 2 \times 10^{-8}$ Pa) equipped with optics of reflection high-energy electron diffraction (RHEED), and an ultraviolet discharge lamp and a rotatable hemispherical electrostatic analyzer for ARUPS. The substrate was mounted on a precision manipulator, via the sample transfer system. A single crystal rod of TaB_2 was grown by a floating-zone technique.[15] A substrate of 1-mm thickness was cut from the rod after the Laue alignment within 0.5° accuracy from the [0001] direction. The substrate surface was mechanically polished with a B_4C powder and a diamond past to a mirror finish. The substrate was heated by electron bombardment from behind. The as-polished surface was first annealed up to 1500 K in 5×10^{-4} Pa of oxygen ambient for 15 min to remove the carbon contamination, and flashed subsequently up to 1500 K below 2×10^{-7} Pa to obtain a clean surface.

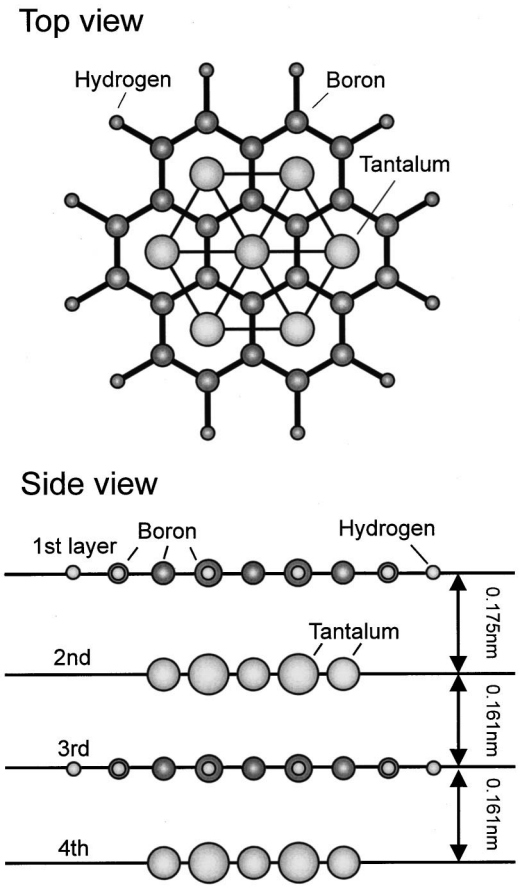

FIG. 1. Projection along the c axis of $Ta_{14}B_{48}H_{24}$ cluster.

III. CALCULATION

Numerical calculations were carried out with use of the SCC-DV-$X\alpha$ method.[16] In this method, the Hartree-Fock-Slater equation for a cluster is selfconsistently solved with use of a localized exchange potential ($X\alpha$ potential). The adjustable (exchange-correlation) parameter α is the only parameter used in this method, and optimum values of α have been determined in the previous work.[16] The value $\alpha=0.7$ is used for all atoms throughout the present calculations.

The biggest $Ta_{14}B_{24}H_{24}$ cluster that was available in our computer was adopted in the DV-$X\alpha$ calculation. Larger clusters should reproduce real bonding nature than smaller clusters more correctly. We also checked cluster size effects, and it is revealed that the results are qualitatively unchanged for smaller clusters. Figure 1 shows the cluster model consisting of first and third graphitic B layers, and second and fourth Ta layers and a c-axis projection of the cluster used for calculation of $TaB_2(0001)$. The spacing of 0.175 nm between the first B and second Ta layers determined by ICISS (Ref. 14) is adopted and the others are same as the bulk crystal (0.161 nm). The bonds of all boron atoms at the edges of graphitic boron layers were terminated with hydrogen atoms so as not to leave any dangling bonds. To avoid the edge effect, we focused on the electronic state of the centered atoms in the cluster.

IV. RESULTS

Figure 2 shows typical ARUPS spectra for $TaB_2(0001)$ surface taken using a He I light (21.2 eV) along $\bar{\Gamma}$-$\bar{K}$ and

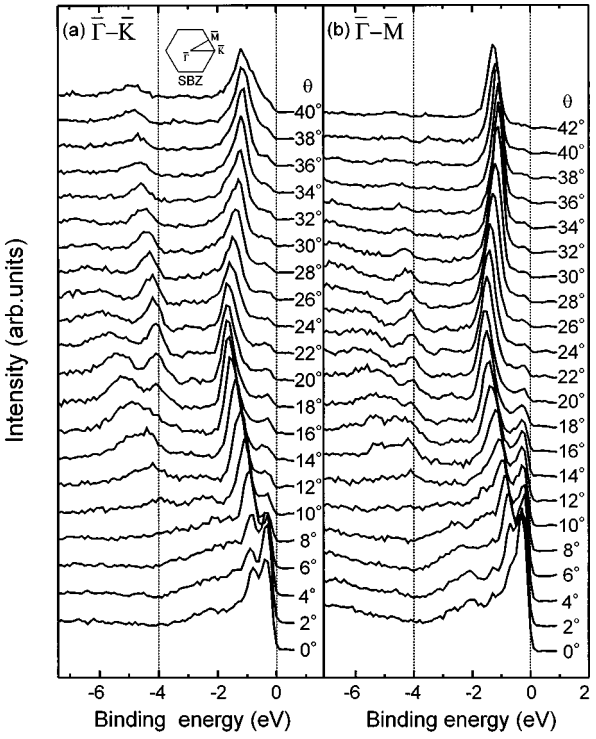

FIG. 2. ARUPS spectra taken along (a) $[11\bar{2}0]$ and (b) $[10\bar{1}0]$ azimuth of the $TaB_2(0001)$ surface terminated with graphitic boron layer.

$\bar{\Gamma}$-$\bar{M}$ symmetry directions. There appear well-developed two peaks in the normal emission spectrum. One is recognized at the Fermi edge and the other at the binding energy of 0.7 eV. The intensity of the peak at the Fermi edge decreases with increasing the emission angle, so that the band would move toward empty state with going toward zone boundary. The other peak has a small dispersion of approximately 1 eV. Two weaker peaks appear in larger emission angle spectra below -4 eV in the binding energy, and exhibit larger dispersion in each direction of $\bar{\Gamma}$-$\bar{K}$ and $\bar{\Gamma}$-$\bar{M}$ symmetry. Figure 3 shows the band structure that is plotted against the momentum component parallel to the surface. In comparison with the two-dimensional (2D) systems having graphitic structure such as a monolayer graphite (MG) and monolayer hexagonal-boron nitride (h-BN),[17,18] the bands located below -4 eV is assignable to the σ bond of the boron layer. However, the parabolic π bond as seen in MG and h-BN is not recognized explicitly in this TaB_2.

Figure 4 shows the calculated energy level structures of the $Ta_{14}B_{48}H_{24}$ and $B_{24}H_{12}$ clusters (same as the first layer of the $Ta_{14}B_{48}H_{24}$ cluster). For simplicity, only energy levels of the a_1, b_1, e_1, and e_2 orbitals corresponding to the $\pi(\pi^*)$-bonds are shown in Fig. 4. The components of the B $2s$,$2p$ orbitals of the B(surface) in the first layer and the B(bulk) in the third layer of $Ta_{14}B_{48}H_{12}$ cluster are also shown in Fig. 4; the length of the horizontal bar represents the B $2s$,$2p$ orbital components in each molecular orbital (MO). The correlation of MO's between the $Ta_{14}B_{48}H_{24}$ cluster and the $B_{24}H_{12}$ cluster are shown by fine lines. The unoccupied $13e_2(\pi^*)$, $13e_1(\pi)$, $7b_1(\pi^*)$, $10a_1(\pi)$,

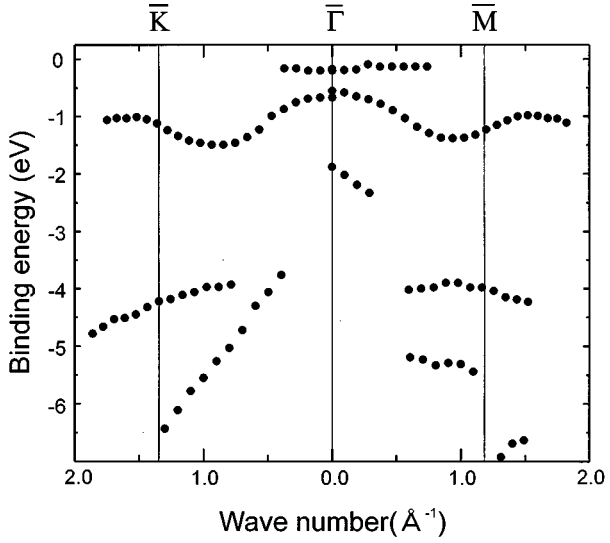

FIG. 3. Electronic band dispersion of $TaB_2(0001)$ surface terminated with graphitic boron layer.

$11e_2(\pi^*)$ and occupied $11e_1(\pi)$, $8a_1(\pi)$ orbitals of the $B_{24}H_{12}$ cluster are split into many orbitals of the $Ta_{14}B_{48}H_{24}$ cluster due to hybridization with the Ta $5d$ orbitals, and some π or π^* orbitals of the $Ta_{14}B_{48}H_{24}$ cluster are lowered in energy and filled with electrons. The some unoccupied orbitals of the $Ta_{14}B_{48}H_{24}$ cluster originated in the $7b_1(\pi^*)$ and $11e_2(\pi^*)$ of the $B_{24}H_{12}$ cluster are filled with electron because of charge transfer form Ta to B. The dominant π-bonds of the B(surface) atoms appear in the range of -3 eV from the highest occupied molecular orbital (HOMO) $(39b_1)$, whereas that of the B(bulk) locates below -4 eV from the HOMO. These facts indicate that the surface boron atoms and the third-layer boron atoms interact strongly with tantalum atoms.

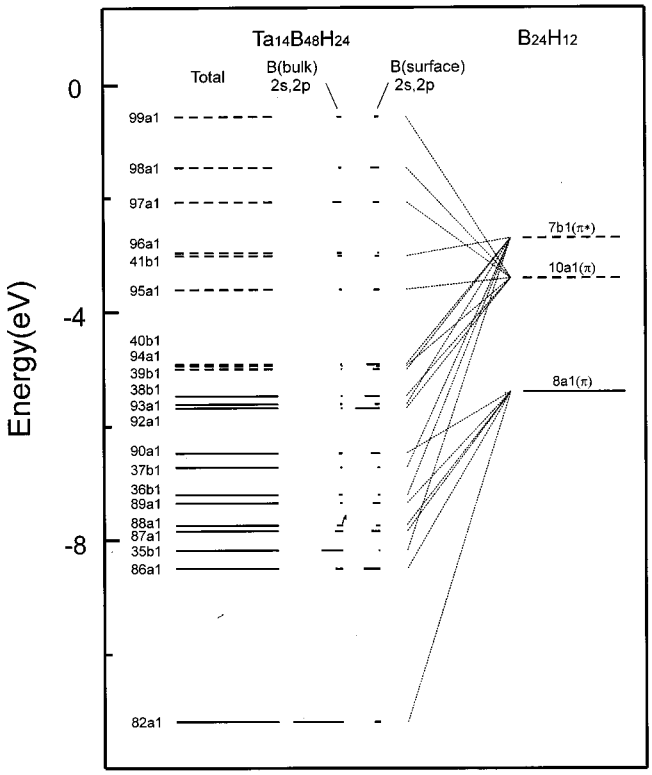

FIG. 4. Energy level structures of $Ta_{14}B_{48}H_{24}$ and $B_{24}H_{12}$ clusters. Solid and dotted lines show occupied and unoccupied levels, respectively.

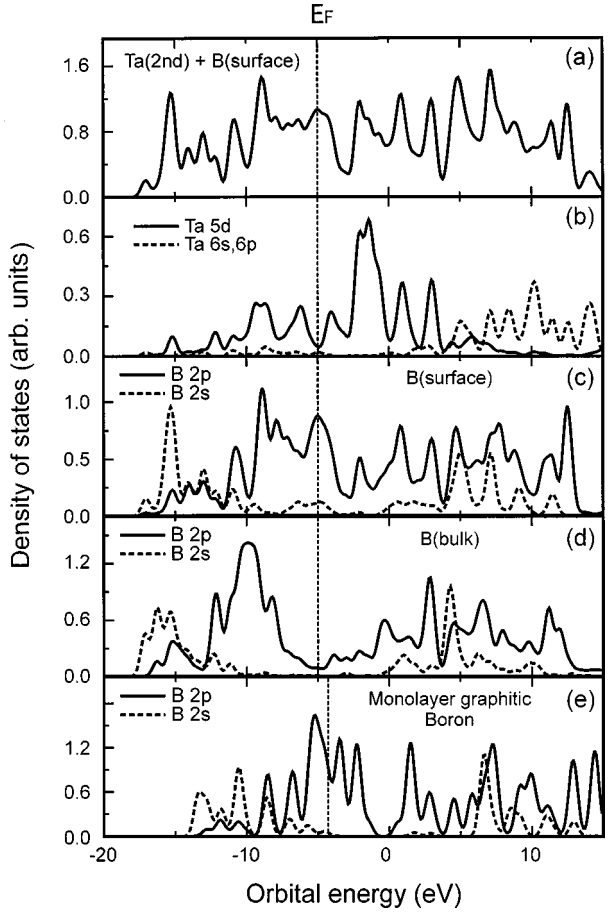

FIG. 5. PDOS and LDOS's of $Ta_{14}B_{48}H_{24}$ and $B_{24}H_{12}$ clusters. The DOS are obtained by spreading the discrete contributions of atomic states on Gaussian function with $\delta = 0.3$ eV.

Figures 5(a), 5(b), and 5(c), 5(d) show the calculated partial and local density of states (PDOS and LDOS) of the Ta(second)+B(surface), the Ta(second), the B(surface) and the B(bulk) of the $Ta_{14}B_{48}H_{24}$ cluster, respectively. The energy gap opens at around 0 ev in the LDOS of the boron in the $B_{24}H_{12}$ cluster [in Fig. 5(e)], whereas it closes in the LDOS of the B(surface) in the $Ta_{14}B_{48}H_{24}$ cluster. The LDOS of the B(surface) and the B(bulk) for the $Ta_{14}B_{48}H_{24}$ cluster is distributed in a wider energy range than that for the $B_{24}H_{12}$ cluster. The peak positions of the LDOS of the B(surface) are modified due to hybridization with the Ta $5d$ orbital. Moreover, the LDOS of the B(bulk) is more strongly modified than that of the B(surface); the LDOS curve of B(bulk) is completely different from that of the $B_{24}H_{12}$ cluster. It should be noticed that the LDOS curve of surface boron layer is similar to the monolayer graphitic boron rather than the third (bulk) boron layer in the $Ta_{14}B_{48}H_{24}$ cluster though the hybridization between B(surface) and Ta(second) occurs largely. Moreover the electronic structure of the boron atoms of the surface should be isoelectronic to graphitic boron layer rather than that of the boron atoms chemisorbed independently on the threefold site of the hexagonal Ta

TABLE I. Net charges and overlap populations for the $Ta_{14}B_{48}H_{24}$ cluster and the $Ta_{13}C_{13}$ cluster.

Cluster	Atoms	Net charges	Overlap populations
$B_{24}H_{12}$	B(surface)-B(surface)		0.78
	B	0.02	
$Ta_{14}B_{48}H_{24}$	B(surface)-B(surface)		0.66
	B(bulk)-B(bulk)		0.63
	B(surface)-Ta(second)		0.11
	B(bulk)-Ta(second)		0.07
	Ta(second)-Ta(second)		0.12
	B(surface)	−0.26	
	B(bulk)	−0.73	
	Ta(second)	1.30	
$Ta_{13}C_{13}$	Ta(first)-C(second)		0.25
	Ta(first)	0.38	
	C(second)	−0.73	

layer. The peaks around −4 eV in the UP spectra, corresponding to the peak at −9.1 eV (−4.1 eV from E_F) in PDOS in Fig. 5(a), is originated mainly from σ-bonds of surface boron atoms hybridized with the Ta $5d$ orbitals. The strong peaks around −1 eV in the UP spectra, assignable to the Ta $5d$ state orbitals can be reproducible in the calculation as seen in Fig. 5(b). Figure 5 clearly indicates that the Ta $5d$ orbitals interact with B π orbitals, so that the peaks around −1 eV in the UP spectra result from hybridization between the Ta $5d$ and B π orbitals. The other peak is expected at the E_F from the B(surface) LDOS in Fig. 5(c). There are, however, no remarkable peaks originated from the Ta(second) and the B(bulk) around E_F. Thus, the peaks located near the E_F in the UP spectra would be caused by the π orbital of the B(surface). The identity of the $2p$ orbital, however, may disappear in the larger binding energy regime due to hybridization with Ta $5d$ state.

The work function (WF) of the graphitic-boron-terminated $TaB_2(0001)$ surface is determined from the width of the UP spectra to be $\phi = 5.9 \pm 0.2$ eV, which is much larger than that of polycrystal boron (4.5 eV). This large value of the WF can be explained by the charge transfer from the second Ta layer to the first B layer. On a $LaB_6(100)$ surface, the charge transfer occurs from La to B atoms and the dipole moment is directed from the surface into the bulk since the outermost layer of the $LaB_6(001)$ surface consists of La atoms.[19,20] As a result, the work function of $LaB_6(001)$ is as small as 2.5 eV. Recently, Hayami *et al.* have reported surface structures of $HfB_2(0001)$ using ICISS. The clean $HfB_2(0001)$ surface, exhibiting a 1×1 structure in RHEED, is terminated by the Hf layer.[21] Moreover, it is claimed that after heating at 2300 K, the boron atoms desorb from the HfB_2 surface, suggesting that B atom is unstable at the $HfB_2(0001)$ surface. As the $HfB_2(0001)$ surface is characterized by metallic property rather than boric hafnium, the WF ($\phi = 4.2 \pm 0.2$ eV) shows almost same as polycrystal hafnium ($\phi = 3.9$ eV). Above WF measurements show that the charge transfer from metal to born plays an important role in electron emission from the surface. Owing to termination of the B atom at the $TaB_2(0001)$ surface, the dipole moment is directed outward, and the work function is increased.

The charge transfer was also confirmed by the DV-$X\alpha$ calculation. Table I summarizes the net charge and overlap population obtained by a Mulliken population analysis. The B(surface) atoms and the B(bulk) atoms possess 0.26 electrons and 0.73 electrons, respectively, from the Ta atoms. The large overlap population between B atoms at the surface shows existence of strong covalency, which is mainly due to the shorter B-B distance (0.179 nm) than the B-Ta distance (0.24–0.25 nm). The B (surface and bulk) atoms have some but not very strong covalency with the Ta atoms, which is almost the same order of that between the Ta-Ta atoms in the second layer.

V. DISCUSSION

TaB_2 has boron layers that are isomorphic to graphite, where of interest is whether the graphitic boron layer is isoelectronic to graphite or not. The charge transfer would bring the solution of the electronic structure of the boron layers. The net charge and WF show that the charge transfer occurs from the Ta to B (in first and third layer), and an excess electron goes into the $2p_z$ orbital of boron. These facts indicate that the boron layers have π bonds between boron atoms. However, the large dispersion of the π-band characteristic of MG or h-BN (Refs. 17 and 18) could not be observed for the TaB_2 as seen in Fig. 3. Band structures of AlB_2 and TiB_2 have been calculated by Freeman *et al.*; π band of simple metal diboride, AlB_2, has a similarity to the graphite π band, while, transition-metal diboride such as TiB_2 does not show isoelectronicity to graphite due to the hybridization between metal d and boron-π orbitals. The B $2p$ state cannot interact with the Ti $5d$ state at the $\bar{\Gamma}$ point but, in going toward the zone boundary it interacts with the Ti d_{xz} and d_{yz} orbitals. The interaction between the boron and the transition metal such as the case for the TiB_2 can be applied to TaB_2. The hybridization between the B π orbital and the Ta $5d$ orbital would modify the parabolic π bonds, which is expected for two-dimensional graphitic boron, and reduces the energy of the π band around $\bar{K}$ and $\bar{M}$ points. Consequently,

the band located around -1 eV in Fig. 3 is strongly modified into the wavy-shape band structure. The positive relaxation between the first boron layer and the second tantalum layer may suggest that the properties of the graphitic boron layer, though hybridized with Ta, are similar to the monolayer graphitic boron. This is the case especially for the first B layer. Table I shows the Mulliken population analyses of the $Ta_{14}B_{48}H_{24}$ cluster and the $Ta_{13}C_{13}$ cluster. The latter simulates the (111) surface of TaC, which has a NaCl-type structure and consists of alternately piled Ta and C layers facing to outside such as the $Ta_{14}B_{48}H_{24}$ cluster; 7Ta, 6C, 6Ta, and 7C atoms in first-fourth layer, respectively. The calculated result shows that B-B bonding has strong covalency, while Ta-B bonding is characterized by the charge transfer from the Ta to the B atoms. Although, the overlap population between the Ta and the B atoms is not large relative to that of Ta-C bond, the calculated DOS and the energy level of the molecular orbital of TaB_2 indicate that large orbital hybridization occurs between the Ta and B.

It is worth while comparing the electronic structure of monolayer boron with those of existing monolayer materials such as the monolayer BN and the MG on metal substrates. The monolayer BN film is physisorbed on metal substrates;[18,22] while the π and the π^* orbitals of MG hybridize with *d* orbitals of metal[23–25] and TMC substrates,[26,27] thereby producing the covalent bonding without significant charge transfer from the substrate to the MG. Owing to the hybridization, the binding energies of the π bond of the MG shift to a higher energy near the edge of the Brillouin zone. In comparison above mentioned monolayer materials, the uniqueness of the graphitic B layer at the $TaB_2(0001)$ surface exists in a large charge transfer from the Ta to B atoms together with some covalency, which is much smaller than that of typical covalent materials such as TMC.

V. SUMMARY

We have investigated the electronic structure of transition-metal diboride $TaB_2(0001)$ surface. The dispersion of the TaB_2 is examined by ARUPS. We found the π band of B around the E_F, which is strongly modified due to interaction with the Ta $5d$ orbital, together with the σ band, which is much less influenced by the substrate. The results are analyzed by SCC-DV-$X\alpha$ calculations. It is concluded that the interaction between the Ta and B layers are characterized by the large charge transfer from Ta to B leading to a large work function of 6 eV, and some interlayer covalency. Such an interaction played by the Ta $5d$ orbital may be important in stabilizing the graphitic B on the Ta layer.

[1] K. E. Spear, in *Phase Diagrams: Materials Science and Technology*, edited by A. M. Alper (Academic, New York, 1970), Vol. 6, p. 91.
[2] D. Emin, Phys. Today **20** (1), 55 (1987).
[3] D. L. Johnson, B. N. Harmon, and S. H. Liu, J. Chem. Phys. **73**, 1898 (1980).
[4] S. H. Liu, L. Kopp, W. B. England, and H. W. Myron, Phys. Rev. B **11**, 3463 (1975).
[5] V. M. Anishchik and N. N. Dorozhkin, Phys. Status Solidi B **160**, 173 (1990).
[6] A. J. Freeman, A. Continenza, M. Posternak, and S. Massidda, in *Surface Properties of Layered Structures*, edited by G. Benedek (Kluwer Academic, Netherlands, 1992), p. 97.
[7] T. Tanaka and Y. Ishizawa, J. Phys. C **13**, 6671 (1980).
[8] T. Tanaka, Y. Ishizawa, E. Bannai, and S. Kawai, Solid State Commun. **26**, 879 (1978).
[9] T. Tanaka and Y. Ishizawa, J. Phys. C **18**, 4933 (1985).
[10] H. Ihara, M. Hirabayashi, and H. Nakagawa, Phys. Rev. B **16**, 726 (1977).
[11] E. Dempsi, Philos. Mag. **8**, 285 (1963).
[12] G. V. Samsonov, Y. M. Goryachev, and B. A. Kovenskaya, J. Less-Common Met. **47**, 147 (1976).
[13] K. E. Spear, J. Less-Common Met. **47**, 195 (1976).
[14] H. Kawanowa, R. Souda, Y. Gotoh, and S. Otani, Phys. Rev. Lett. **81**, 2264 (1998).
[15] S. Otani and T. Tanaka (unpublished).
[16] H. Adachi, M. Tsukada, and C. Satoko, J. Phys. Soc. Jpn. **45**, 875 (1978).
[17] B. S. Itchkawitz, P. F. Lyman, G. W. Ownby, and D. M. Zehner, Surf. Sci. **318**, 395 (1994).
[18] A. Nagashima, N. Tejima, Y. Gamou, T. Kawai, and C. Oshima, Phys. Rev. Lett. **75**, 3918 (1995).
[19] C. Oshima, E. Bannai, T. Tanaka, and S. Kawai, J. Appl. Phys. **48**, 3925 (1977).
[20] R. Nishitani, M. Aono, T. Tanaka, C. Oshima, S. Kawai, H. Iwasaki, and S. Nakamura, Surf. Sci. **93**, 535 (1980).
[21] W. Hayami, R. Souda, T. Aizawa, and T. Tanaka, Surf. Sci **415**, 433 (1998).
[22] A. Nagashima, N. Tejima, Y. Gamou, T. Kawai, and C. Oshima, Surf. Sci. **357/358**, 307 (1996).
[23] R. Rosei, S. Modest, F. Sette, C. Quaresima, A. Savoia, and P. Perfetti, Solid State Commun. **46**, 871 (1983).
[24] K. Yamamoto, M. Fukushima, T. Osaka, and C. Oshima, Phys. Rev. B **45**, 11 358 (1992).
[25] A. Nagashima, N. Tejima, and C. Oshima, Phys. Rev. B **50**, 17 487 (1994).
[26] A. Nagashima, K. Nuka, H. Itoh, T. Ichinokawa, and C. Oshima, Surf. Sci. **291**, 93 (1993).
[27] K. Kobayashi and M. Tsukada, Phys. Rev. B **49**, 7660 (1994).